Probabilistic egomotion from a statistical framework

Hitesh Shah and Arvind Lakshmikumar
Sarnoff Innovative Technologies Pvt. Ltd.
Bangalore, India
(hshah, alakshmikumar)@sarnoff.com

Abstract

Traditional egomotion estimation algorithms have largely depended on deterministic feature correspondences to infer information about the camera and have been oblivious to the scene geometry by treating scenes with varying projectivities uniformly. This paper builds on the statistical framework of the joint feature distribution (JFD) which models the joint probability distributions of the positions of corresponding features in different images. This framework explicitly gives probabilistic correspondence search regions that can be stably estimated for the whole range of planar, shallow and deep scenes using relatively few correspondences. These joint probability distributions are constrained by the epipolar constraint to yield a distribution over all feasible egomotions. The paper also compares the proposed method against existing well-known methods and quantifies the improvements in the egomotion estimates.

1   Introduction

Egomotion estimation is a critical step while analyzing scenes from moving cameras. The aim of egomotion computation is to estimate translation and rotation, i.e. external camera parameters, the camera undergoes while capturing the sequence of images. An array of methods to estimate egomotion of moving cameras with respect to both stationary and dynamic scenes using a deterministic framework have been proposed. Tian et. al [15] and Armangue et. al [1] summarize these methods and group them based on their underlying principles.

Kanatani's method [7] based on the epipolar constraint has been the basis for several linear egomotion algorithms. The Essential matrix which serves as the support for the epipolar constraint faithfully captures the epipolar geometry between the camera views and can be estimated using the linear 8 point algorithm [5], or the state of the art 5 point algorithm [11] [9].

The above mentioned methods directly use feature correspondences between images and use these matches to robustly estimate the Essential matrix. However, given the vagaries in scene structure, extracting dense feature correspondences between images is not always possible. This paper builds on the premise that robust egomotion estimation does not have to rely on dense, deterministic image correspondences. Instead, a probability distribution of the uncertainties in correspondences would be sufficient. This paper uses the joint feature distributions (JFD) [17] to build these probability distributions. The JFD

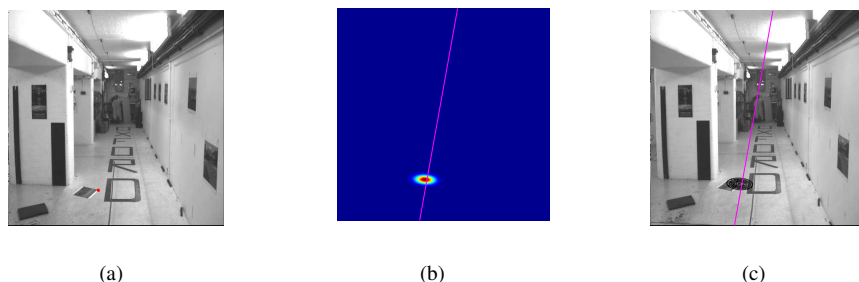| (a) | (b) | (c) |

Figure 1: Joint Feature Distribution (JFD) and Epipolar line : (a) shows the point under consideration marked in red. (b) shows the corresponding epipolar line (calculated using the ground truth data) and probability distribution of the point correspondence using JFD, (c) the iso-contour plot of the probability distribution and the epipolar line overlaid on the second image.

is used to predict feature correspondences between images. Probability distribution for the Essential matrix is computed from the JFD by evaluating how well each tentative Essential matrix's epipolar lines fit the feature correspondence distribution.

The motivating application for this paper is to estimate the motion of a vehicle using a rigidly attached camera. In some cases this task becomes difficult as multiple hypotheses may fit the epipolar geometry for e.g. the camera view may be of shallow scene or a deep scene or a largely planar scene. If an incorrect hypothesis is chosen, the estimated motion can break and lead to an incorrect state from which the motion estimate is unlikely to recover. The uncertainty estimates from the joint feature distributions provide us with a mechanism to choose the best hypothesis from the space of available choices.

The paper is organized as follows. Section 2 motivates the requirement to represent the correspondence information probabilistically and later describes our chosen method of probabilistic representation. Section 3 goes on to describe the method used to extract egomotion information from this probabilistic representation. Section 4 compares and contrasts our approach with other known methods in literature. The paper ends with a summary on future work.

2 Probabilistic Correspondence

Estimation of the correspondences of features between images is a difficult task. Traditionally, a feature detector (e.g. the Harris corner detector [4]) is used to find points whose correspondence is most easily established. Then, matching techniques are used to find probable matches between the feature points in both images (e.g. normalized cross correlation, or SIFT features [10]).

Most feature extraction and subsequent matching process are hindered by noise, scale, orientation changes, aperture effect, and repetitive scene structure. The ambiguities arising from these effects would cause feature based matching techniques to reject true feature points as weak ones or as outliers. A probability distribution gives us a mechanism for representing this ambiguity.

There is a good deal of literature regarding representing these ambiguities explicitly using probabilistic methods. For the purpose of computing optical flow [2] estimates traditional flow vectors at each point, by first estimating flow probability distributions, and then combining this information using spatiotemporal support regions. For the same

problem [14] creates a probability distribution over the optical flow by assuming image gradients are corrupted by a Gaussian noise model. These distributions are then used to estimate optical flow vectors with higher accuracy. Object tracking has also been addressed [13] using the probabilistic notions of correspondence. In [3] the authors proposes a method to compute correspondence probability distributions using Gabor filters that are tuned to different orientations and scales. They use the fact that for a given filter, matching points will have matching phase. They further illustrate the application of this approach to the problem of egomotion estimation. However, their method is only suitable for situations with limited rotation or scale change and does not have a mechanism to counter the effects of varying projectivities in a scene. Also, in presence of regularly repetitive texture, the responses of the Gabor filter bank are identical at multiple places and this would lead to problems during the egomotion estimation phase.

Joint Feature distribution (JFD) [17] allows statistical representation of feature correspondences in different image as a probability distribution. The probability distribution serves to capture the correspondences entirely as conditioning on a feature gives tight probabilistic correspondence search regions for the remaining ones. As concisely stated in [17], JFDs are descriptive statistical models rather than normative geometric ones: they aim to summarize the observed behavior of the given training correspondences, not to rigidly constrain them to an ideal predefined geometry.

The problem we address in this paper is egomotion estimation of a camera mounted on a moving vehicle. This application involves situations with deep scale and steep rotation changes. The JFD's offer a principled mechanism to generate the joint distributions of feature points that undergo these changes. The uncertainty distributions generated by the JFD are then used as the input to our egomotion algorithm.

2.1 Joint Feature Distributions

Noisy image projections $x_i | i = 1 \cdots m$ of a fixed 3D feature f can be modeled as probability distributions $p(x_i | f)$ centered on $f's$ true projections. If f varies across some 3D features with distribution $p(f)$, the joint feature distribution (JFD) of the resulting population of image features is

$$\mathbf{p}(x_1, \cdots, x_m) = \int p(x_1, \cdots, x_m | f) p(f) df. \tag{1}$$

JFDs are image-based models originally derived from 3D quantities (in this case, the 3D feature prior $p(f)$ and the projection models $p(x_i | f)$), but typically estimated from observed image correspondences.

Let $\mathbf{x} = (x, y, 1)$ and $\mathbf{x}' = (x', y', 1)$ be the homogeneous coordinates of the corresponding points (correspondences established using traditional feature detection and matching) in the image im_1 and im_2. Then a joint image vector is defined as

$$\mathbf{t} = \mathbf{x} \otimes \mathbf{x}' = (xx', xy', x, yx', yy', y, x', y', 1). \tag{2}$$

Given N correspondences between images $im1$ and $im2$ a 9 x N matrix $\mathbf{M}$ is obtained by stacking the joint image vectors. Thus $\mathbf{M} = [\mathbf{t_1} \ \mathbf{t_2} \ ... \ \mathbf{t_N}]$. The homogeneous scatter matrix $\mathbf{V}$ is

$$\mathbf{V} = \frac{1}{N} \sum_p \mathbf{t}_p \mathbf{t}_p^T = \frac{1}{N} \mathbf{M} \mathbf{M}^T.$$

The fundamental matrix uses just the smallest eigenvector of $\mathbf{M}\mathbf{M}^T$ whereas the JFD model captures the underlying uncertainty using an appropriately-weighted average over all of the eigenvectors $((\mathbf{M}\mathbf{M}^T)^{-1})$. Conditioning the JFD gives compact correspondence search regions consistent with all the likely models in the average. The JFD information matrix that forms the basis of our probabilistic representation is $\mathbf{W} \approx \mathbf{V}^{-1}$. Now the probability of a point $\mathbf{x} = (x, y, 1)$ to correspond to $\mathbf{x}' = (x', y', 1)$ using JFD is given by

$$\mathbf{p}(\mathbf{x}, \mathbf{x}') = \mathbf{k_i}e^{\frac{-1}{2}\mathbf{t}^T \mathbf{W} \mathbf{t}}, \tag{3}$$

where $\mathbf{t}$ is as defined by equation (2) and $\mathbf{k_i}$ is a constant to normalize the distribution.

2.2 Reducing the probability distribution

The joint image vector can be reformulated as follows

$$
\begin{aligned}
\mathbf{t} &= \mathbf{x} \otimes \mathbf{x}' \\
&= [xx', xy', x, yx', yy', y, x', y', 1]_{9 \times 1}^T \\
&= \begin{bmatrix} xI_3 \\ yI_3 \\ I_3 \end{bmatrix}_{9 \times 3} \bullet \begin{bmatrix} x' \\ y' \\ 1 \end{bmatrix}_{3 \times 1}
\end{aligned}
$$

where I_3 is a 3×3 identity matrix. Let $\mathbf{Q} = [xI_3 \quad yI_3 \quad I_3]^T$, thus $\mathbf{t} = \mathbf{Q} \cdot \mathbf{x}'$. Using equation (3), the probability for correspondence between $\mathbf{x}$ and $\mathbf{x}'$ is given by

$$
\begin{aligned}
\mathbf{p}(\mathbf{x}, \mathbf{x}') &= \mathbf{k_i}e^{\frac{-1}{2}\mathbf{x}'^T \mathbf{Q}^T \mathbf{W} \mathbf{Q} \mathbf{x}'} \\
&= \mathbf{k_i}e^{\frac{-1}{2}\mathbf{x}'^T \mathbf{A} \mathbf{x}'}
\end{aligned} \tag{4}
$$

where $\mathbf{A} = \mathbf{Q^T W Q}$.

Figure 1 shows the probability distribution obtained using the equation (4). It can be noted that the probability distribution models the correspondence and the associated uncertainty well.

3 Egomotion Estimation

Egomotion of a moving camera is in essence the relative geometry between subsequent camera views. This geometry is well captured by the 3×3 homogeneous Essential matrix. Consider a camera with constant intrinsic matrix $\mathbf{K}$ observing a static scene. Two corresponding image points $\mathbf{x}$ and $\mathbf{x}'$ are then related by a fundamental matrix $\mathbf{F}$:

$$\mathbf{x}'^{\mathbf{T}}\mathbf{F}\mathbf{x} = \mathbf{0} \tag{5}$$

A valid $\mathbf{F}$ must also satisfy the cubic singularity condition $\det \mathbf{F} = 0$. If the camera is fully-calibrated with $\mathbf{K}$ as the internal camera calibration matrix, then the fundamental matrix is reduced to an essential matrix denoted by $\mathbf{E}$, and the new equation is:

$$\mathbf{K}^{-\mathbf{T}}\mathbf{E}\mathbf{K}^{-\mathbf{1}} = \mathbf{F}. \tag{6}$$

The Essential matrix $\mathbf{E}$ is a representation of the motion (translation and rotation, up to a scale), it has only five degrees of freedoms. Consequently, to be a valid essential matrix $\mathbf{E}$, it must further satisfy two more constraints, which are characterized by

$$2\mathbf{E}\mathbf{E}^{\mathbf{T}}\mathbf{E} - Tr(\mathbf{E}\mathbf{E}^{\mathbf{T}})\mathbf{E} = \mathbf{0}, \tag{7}$$

where $Tr(\mathbf{A})$ is the trace of the matrix $\mathbf{A}$. The above constraints can also be satisfied by formulating the Essential matrix in terms of the translation and rotation the camera undergoes. A unit length vector for translation can be uniquely represented by a point on the unit sphere. Thus it can be characterized by two parameters (α, β).

$$\mathbf{T} \quad = \quad [\sin(\alpha)\cos(\beta), \sin(\alpha)\sin(\beta), \cos(\alpha)]^T$$

The rotation is represented by a vector $\omega = [x, y, z]^T$. Here the angle of rotation is $\theta = \sqrt{x^2 + y^2 + z^2}$ and the axis of rotation is $\hat{\omega} = \omega/\theta = [\hat{x}, \hat{y}, \hat{z}]^T$. Thus given the 5 parameters (α, β, x, y, z) the essential matrix can be composed as follows.

$$\mathbf{E} \quad = \quad [\mathbf{T}]_{\times}\mathbf{R}(\omega), \tag{8}$$

where $\mathbf{R}(\omega)$ is the rotation matrix corresponding to the rotation vector ω.

3.1   Probability of egomotion given a point

Given a correspondence probability distribution for a single point $\mathbf{x}$, the probability of a given hypothesis (α, β, x, y, z), and hence $\mathbf{E}$ (by equation (8)), is taken to be maximum probability $\mathbf{p}(\mathbf{x}, \mathbf{x}')$ such that $\mathbf{x}$ and $\mathbf{x}'$ satisfy the epipolar constraint, i.e. $\mathbf{x}^{\mathbf{T}}\mathbf{F}\mathbf{x}' = 0$ where $\mathbf{F}$ is the fundamental matrix given by equation (6). This translates to

$$\mathbf{P_x}(\mathbf{E}) \quad = \quad \mathbf{max_{x'}} \ \mathbf{p}(\mathbf{x}, \mathbf{x}') \tag{9}$$
$$\text{subject to } \mathbf{x}^{\mathbf{T}}\mathbf{F}\mathbf{x}' = \mathbf{0}$$

All $\mathbf{x}'$ which satisfy the epipolar constraint lie on the line given by $\mathbf{l} = \mathbf{F}\mathbf{x}$. Consider two points on the epipolar line $\mathbf{l} = [l_1, l_2, l_3]$.

$$p1 = [0, \frac{-l_3}{l_2}, 1] \quad p2 = [\frac{-l_3}{l_1}, 0, 1]$$

Any point on the epipolar line can thus be represented as

$$\mathbf{x}'(\mathbf{t}) \quad = \quad o + \mathbf{t}d, \tag{10}$$

where $o = p2$ and $d = (p1 - p2)$.

Equation (9) can be reformulated using equation (10) along with equation (4) to have new parameterization of $\mathbf{t}$ which inherently incorporates the epipolar constraint. This essentially converts the constrained maximization over $\mathbf{x}'$ to an unconstrained maximization over $\mathbf{t}$.

$$\mathbf{P_x}(\mathbf{E}) \quad = \quad \mathbf{max_t} \ \mathbf{p}(\mathbf{x}, \mathbf{x}'(\mathbf{t}))$$
$$= \quad \mathbf{max_t} \ \mathbf{k_i}e^{\frac{-1}{2}\mathbf{x}'(\mathbf{t})^{\mathbf{T}}\mathbf{A}\mathbf{x}'(\mathbf{t})} \tag{11}$$

Maxima for the equation (11) will occur for a value of $\mathbf{t}$ which minimizes $\mathbf{x'(t)^T A x'(t)}$. Thus

$$\tilde{\mathbf{t}} \;=\; \mathbf{arg\ min_t}\ (o+\mathbf{t}d)^T A(o+\mathbf{t}d). \qquad (12)$$

Minimizing the equation (12) we have $\tilde{\mathbf{t}} = -\frac{o^T \mathbf{A}d}{d^T \mathbf{A}d}$. Hence

$$\mathbf{P_x(E)} \;=\; \mathbf{k_i} e^{\frac{-1}{2}\check{\mathbf{x}}^T \mathbf{A}\check{\mathbf{x}}}, \qquad (13)$$

where $\check{\mathbf{x}} = o - \frac{o^T \mathbf{A}d}{d^T \mathbf{A}d}d$.

3.2   Probability distribution of egomotion

The probability of egomotion computed over all the points is given by combining the information given by all points. Hence

$$\mathbf{P(E)} = \mathbf{C} \prod_{\mathbf{i}}^{\forall\ \mathbf{points}} \mathbf{P_{x_i}(E)}, \qquad (14)$$

where $\mathbf{C}$ is the normalizing constant for the distribution. Ideally we would like to consider all the points on the image, not only the points for which the correspondence was established during the initial JFD calculation phase in the above equation. However, empirically we have found that taking even few equally spaced points on a grid results in an accurate probability distribution of $\mathbf{E}$ and calculated egomotion (refer section 4).

Using equation (13) the above equation becomes

$$\mathbf{P(E)} = \mathbf{C} \prod_{\mathbf{i}}^{\forall\ \mathbf{points}} \mathbf{k_i} e^{\frac{-1}{2}\check{\mathbf{x}}_{\mathbf{i}}^T \mathbf{A}\check{\mathbf{x}}_{\mathbf{i}}}.$$

To estimate the egomotion $\tilde{\mathbf{E}}$, we find the motion parameters (α, β, x, y, z) which maximize the $\mathbf{P(E)}$. Hence

$$
\begin{aligned}
\tilde{\mathbf{E}} \;&=\; \mathbf{arg\ max_E}\ (\mathbf{C} \prod_{\mathbf{i}}^{\forall\ \mathbf{points}} \mathbf{k_i} e^{\frac{-1}{2}\check{\mathbf{x}}_{\mathbf{i}}^T \mathbf{A}\check{\mathbf{x}}_{\mathbf{i}}}) \\
&=\; \mathbf{arg\ max_E}\ (\prod_{\mathbf{i}}^{\forall\ \mathbf{points}} e^{\frac{-1}{2}\check{\mathbf{x}}_{\mathbf{i}}^T \mathbf{A}\check{\mathbf{x}}_{\mathbf{i}}}) \\
&=\; \mathbf{arg\ min_E}\ (\sum_{\mathbf{i}}^{\forall\ \mathbf{points}} \check{\mathbf{x}}_{\mathbf{i}}^T \mathbf{A}\check{\mathbf{x}}_{\mathbf{i}}) \qquad (15)
\end{aligned}
$$

In practice the optimization of the equation (15) over this 5 dimensional space is carried out as follows.

- Evaluate $\mathbf{P(E)}$ at 250 random samples in 5D motion space.

- Sort in descending order and select top 50 samples.

- Use them as seed points to start nonlinear search for optimal parameter set.

- Select the parameter set which gives minimum value for $\mathbf{P(E)}$ from the resulting parameter set of above nonlinear search.

<div align="center">(a)</div>
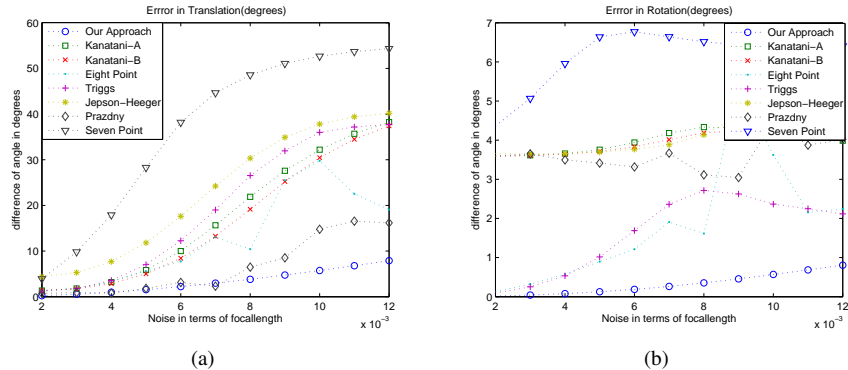<div align="center">(b)</div>

Figure 2: Comparison of (a) error in the translational and (b) error in rotational component of the estimated egomotion using various approaches with varying amounts of noise levels in the correspondences.

4 Experimental results

We compare the performance of the proposed approach with several well established methods on real as well as synthetic data . The error metric for estimated translation **T** with respect to the ground truth translation $\tilde{\mathbf{T}}$ is computed as

$$e_T = \cos^{-1}(\mathbf{T}'\tilde{\mathbf{T}}).$$

Similarly, the error metric for estimated rotation matrix **R** with respect to the ground truth rotation matrix $\tilde{\mathbf{R}}$ is computed as

$$e_R = \cos^{-1}\left(\frac{Tr(\mathbf{R}'\tilde{\mathbf{R}}) - 1}{2}\right).$$
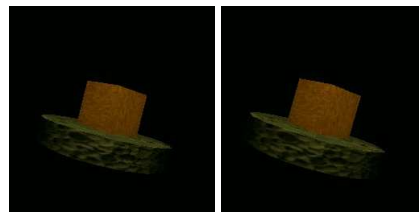
Since the internal camera parameters are assumed to be known in all the experiments on synthetic data, we have used normalized coordinates for the correspondences.

In general for minimization in 5D space it is hard to guarantee of convergence. However, due to the Gaussian nature of correspondence and parameterization of equation (15) very few local minima were observed. This coupled with evenly distributed multiple seed points in the 5D space resulted in convergence to the global minima each time in our experiments.

4.1 Synthetic data

For synthetic data, 100 3D points were randomly selected in front of the camera covering the field of view. These points were then projected on a image considering a unit focal length camera at canonical position on origin. The camera undergoes $\tilde{\mathbf{T}}$ translation and $\tilde{\mathbf{R}}$ rotation and the points are re-projected, using the new camera position, on the image. The correspondences thus generated are then perturbed by zero mean Gaussian noise to quantify the performance of various algorithms with increasing levels of noise. In our experiments, the noise variance was varied from 2×10^{-3} to 12×10^{-3} (in units of focal length) which approximately translates to 0.5 pixels to 2.5 pixels for a 512×512 image with unit focal length and $90°$ field of view.

Figure 2 shows the performance of the proposed approach on noisy data in comparison with Kanatani-A [7], Kanatani-B [8], Jepson-Heeger [6], Prazdny [12], Triggs [16], Eight

Approach	Error in translation	Error in rotation
Proposed approach	1.0856	0.0026
Domke's approach	1.1786	0.3009
Eight point approach	2.9182	1.0144

(c)

Figure 3: Translation and rotational error in degrees for the estimated egomotion between cameras of the image (a) and (b). The comparision table is shown in (c).

Point [5], and Seven Point [18] approaches. Implementation of the Kanatani-A, Kanatani-B, Jepson-Heeger, Prazdny have been adapted from the MATLAB toolbox given by Tian et. al [15]. The Triggs method is based on the projective factorization approach proposed by [16] to calculate the projection matrices for the two cameras. These are then decomposed to obtain the egomotion. On similar lines, the Eight point and Seven point algorithms are used to obtain the Fundamental matrix. Since the image coordinates are normalized in our case, we compute the Essential matrix which is then factorized to obtain the solution for the egomotion. It can be observed from the comparisons in Figure 2 that the egomotion estimates using the proposed probabilistic approach performs better then deterministic approaches which can be attributed to the ability of the probability distribution to handle noise in the correspondences.

4.2   Synthetic and Real Images

We have used synthetic image from SOFA [1] for evaluating the performance of the proposed method. The pairs of images in which the camera undergoes translation and rotation have been selected for this set of experiments.

Besides the comparisons in Figure 2, we also compare our results with the only other method, Domke et. al [3] that uses probabilistic correspondences for egomotion estimation. We use an available implementation [2] of this method for our evaluation. The table in the Figure 3 show some results of our experimentation. The comparisons shown are between the proposed method, Domke's method and the linear approach. For the proposed and linear approaches, point correspondences are obtained between images using SIFT based matching. For the Eight point approach, fundamental matrix is calculated based on this matches using RANSAC. Essential matrix obtained from the fundamental matrix and is decomposed to obtain the solution for egomotion. It can observed that the proposed approach outperforms both the linear and Domke's method.

In the case of real images, SIFT based feature matching was used to generate the point correspondences which are then used to calculate the JFD. To show the validity of our approach for real images we have calculated the epipolar lines based on the egomotion

---

[1] SOFA synthetic sequences courtesy of the Computer Vision Group, Heriot-Watt University (http://www.cee.hw.ac.uk/ mtc/sofa)

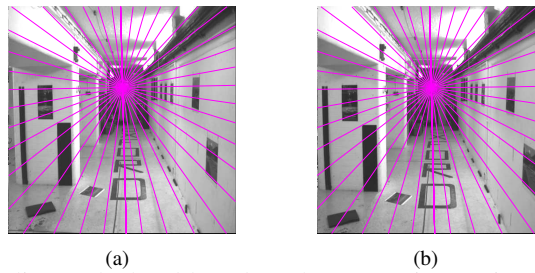[2] http://www.cs.umd.edu/ domke/egomotion/

| (a) | (b) |

Figure 4: Epipolar lines calculated based on the egomotion, estimated by proposed approach, overlaid over the real images in (a) and (b).

evaluated using the proposed approach. Figure 4 shows the epipolar lines overlaid on the respective images.

We also have experimented by varying the number of points in the equation (14) and have found that taking few equally spaced points on the image gives accurate results. As observed in Figure 5 increasing the number of equally spaced point beyond 36 (i.e. grid size= 6) does not yield a significant improvement in the accuracy of the estimated egomotion.

5   Conclusion and Discussions

In this paper, we have described a method to compute the egomotion of a moving camera using the statistical concept of joint feature distributions (JFD). The JFD's captured the statistics of a given collection of training correspondences and we used them to build a dense set of correspondences of the same kind. In this work, we focussed on using the JFD to predict correspondences and then used the epipolar constraint to find a probability distribution for the egomotion.

The JFD contains all the information regarding the uncertainties in egomotion. When the scene is decidedly deep, the fundamental matrix is well defined and we have a homogeneous covariance matrix for the family of epipolar lines associated with a given point x_i and the corresponding epipole e. So, the translation direction (e) and the rotation information (available from the fundamental matrix and e) can be calculated. For shallow scenes, the uncertainty in homographies is well characterized by the JFD information matrix (its inverse contains the homogeneous information of the homography) and this can be decomposed into translation and rotation components.

For scenes with varying degrees of projectivities (or collections of planes), a mixture of shallow JFD's (their shared eigenvector) would allow us to characterize the scene. We are currently exploring approaches that would allow us to compute the uncertainty in egomotion directly from this information without imposing the additional epipolar constraints.

References

[1] X. Armangu, H. Arajo, and J. Salvi. A review on egomotion by means of differential epipolar geomety applied to the movement of a mobile robot. *Pattern Recognition*, 21, 2003.

[2] W.F Clocksin. A new method for computing optical flow. In *Proceedings of British Machine Vision Conference*, 2000.
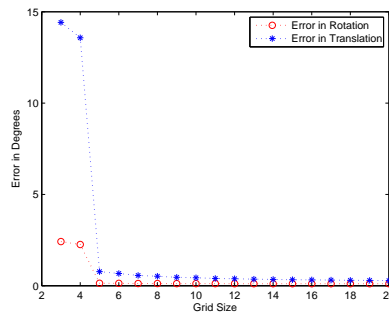
Figure 5: Improvement in accuracy of the estimated egomotion with increase in number of points under consideration in the proposed approach. *n* grid size means a equally spaced grid of $n \times n$ points on the image

[3] J. Domke and Y. Aloimonos. A probabilistic framework for correspondence and egomotion. In *ICCV Workshop on Dynamic Vision*, 2005.

[4] C.G Harris and M Stephens. A combined corner and edge detector. In *AVC*, 1988.

[5] Richard Hartley. In defense of the eight-point algorithm. *IEEE Transactions on Pattern Analysis and Machine Intelligence*, 19, 1997.

[6] Allan D. Jepson and David J. Heeger. Linear subspace methods for recovering translational direction. In *Proceedings of the 1991 York conference on Spacial vision in humans and robots*, 1993.

[7] K. Kanatani. Unbiased estimation and statistical analysis of 3-d rigid motion from two views. *IEEE Trans. Pattern Anal. Mach. Intell.*, 15, 1993.

[8] Kenichi Kanatani. 3-d interpretation of optical flow by renormalization. *Int. J. Comput. Vision*, 11, 1993.

[9] Hongdong Li and Richard Hartley. 5-point motion estimation made easy. In *Proceedings of the International Conference on Pattern Recognition*, 2006.

[10] David Lowe. Distinctive image features from scale-invariant keypoints. In *International Journal of Computer Vision*, 2004.

[11] David Nister. An efficient solution to the five-point relative pose problem. In *Proceedings of Computer Vision and Pattern Recognition*, 2003.

[12] K. Prazdny. Egomotion and relative depth map from optical flow. *Biological Cybernetics*, 36, 1980.

[13] Y Rosenberg and M Werman. Representing local motion as a probability distribution matrix applied to object tracking. In *Proceedings of Computer Vision and Pattern Recognition*, 1997.

[14] E.P Simoncelli, E.H Adelson, and D.J Heeger. Probability distributions of optical flow. In *Proceedings of the IEEE Conference on Computer Vision and Pattern Recognition*, 1991.

[15] Tina Y. Tian, Carlo Tomasi, and David J. Heeger. Comparison of approaches to egomotion computation. In *Proceedings of the Conference on Computer Vision and Pattern Recognition*, 1996.

[16] Bill Triggs. Factorization methods for projective structure and motion. In *Proceedings of the IEEE Conference on Computer Vision and Pattern Recognition*, 1996.

[17] Bill Triggs. Joint feature distributions for image correspondence. In *ICCV*, 2001.

[18] Zhengyou Zhang. Determining the epipolar geometry and its uncertainty: A review. Technical Report 2927, Sophia-Antipolis Cedex, France, 1996.